Available online at www.sciencedirect.com
SCIENCE DIRECT
Polymer 47 (2006) 972–981
polymer
www.elsevier.com/locate/polymer

Elastomer polymer brushes on flat surface by bimolecular surface-initiated nitroxide mediated polymerization

Julien Parvole [a], Jean-Pierre Montfort [a], Günter Reiter [b], Oleg Borisov [a], Laurent Billon [a,*]

[a] *Laboratoire de Physico-Chimie des Polymères, UMR 5067—Université de Pau et des Pays Adour, Hélioparc Pau-Pyrénées, 2 Av. P. Angot, 64053 Pau, Cedex 09, France*

[b] *Institut de Chimie des Surfaces et Interfaces, UPR 5069—Université de Haute Alsace,15, rue Jean Starcky, BP 2488, 68057 Mulhouse, Cedex, France*

Received 13 July 2005; received in revised form 19 December 2005; accepted 20 December 2005

Abstract

The method of formation of well-defined polymer brushes based on the nitroxide mediated polymerization (NMP) of *n*-butyl acrylate (BA) initiated from a self-assembled mono-layers (SAMs) of an azoic initiator in the presence of a stable nitroxide radical is described. After preliminary qualitative characterization by X-ray photoelectron spectroscopy, the samples were studied by ellipsometry in order to determine the dry film thickness (initiator and polymer) and the grafting density of macromolecular chains. It is demonstrated, that in the presence of stable counter radical SG1, acting as chain growth moderator, the surface initiated NMP exhibits a living/controlled character permitting to control architectural parameters (e.g. degree of polymerization) of elastomer grafted polymer chains. The possibility to use the living control character of this type of polymerization to re-initiate grafted chains in order to increase the thickness of an elastomer thin film with conservation of the brushes regime has been demonstrated.
© 2006 Elsevier Ltd. All rights reserved.

Keywords: Surface-initiated nitroxide mediated polymerization; Elastomer; Polymer brushes

1. Introduction

Due to its proficiency to lead to macromolecules with well-defined structure and macromolecular dimensions, controlled/living radical polymerization (CRP), and in particular nitroxide mediated polymerization (NMP), has been extensively described since almost ten years. The CRP is based on a rapid dynamic equilibrium between a minute amount of growing free radicals and a large majority of the dormant species [1]. The dormant chains may be alkyl halides, as in atom transfer radical polymerization (ATRP) [2–4] or alkoxyamine [5–14] as in our case, in NMP, or stable free radical polymerization (SFRP).

More recently, NMP was used as a tool for preparation of well-defined grafted polymer mono-layers on silica surfaces (vinyl and acrylic monomers) [10–14]. Developments in the elaboration of new materials have enabled the synthesis of novel polymer brushes comprising a wide range of organic polymers tethered onto spherical or flat surfaces [15]. By definition, polymer brushes are assemblies of polymer chains which are tethered by one end to a surface or an interface. Due to sufficiently dense grafting, polymer chains in the brush are crowded and stretch away from the surface or interface to minimize the free energy of steric repulsion. The fabrication of patterned high-density polymer grafted surfaces is accomplished by the grafting from approach. In this case, performed functionalized azoic [10a–d,11] and peroxide [14] initiators (bimolecular system), or alkoxyamine [10e,11,12] initiators (unimolecular system) are synthesized and covalently attached to a variety of solid surfaces, e.g. silicon substrates or colloidal particles. As a second step, a radical polymerization is initiated from the surface under controlled conditions (Scheme 1) [10–14].

Moreover, this approach can be used to study end-grafted polymer monolayers in 'mushroom' regime by AFM-based single molecule force spectroscopy [16].

In the present paper, we start with the description of the formation of self-assembled mono-layers obtained with trichloro (ATCl) and monochloro (AMCl) functionalized initiator (Scheme 2(b)). Then we discuss the formation of poly(*n*-butyl acrylate) (PBA) brushes by surface-initiated

* Corresponding author. Tel.: +33 5 59 40 76 09; fax: +33 5 59 40 76 23.
E-mail addresses: julien.parvole@univ-pau.fr (J. Parvole), jean-pierre.montfort@univ-pau.fr (J.-P. Montfort), g.reiter@univ-mulhouse.fr (G. Reiter), oleg.borisov@univ-pau.fr (O. Borisov), laurent.billon@univ-pau.fr (L. Billon).

0032-3861/$ - see front matter © 2006 Elsevier Ltd. All rights reserved.
doi:10.1016/j.polymer.2005.12.072

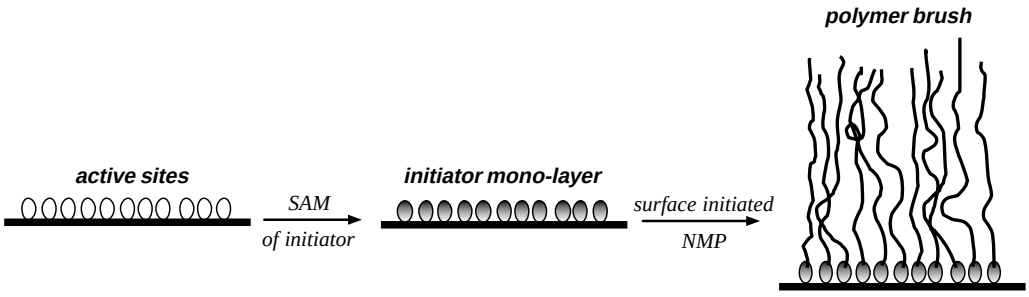

Scheme 1. Schematic representation of polymer brush formation.

NMP with a bimolecular system azoic initiator/SG1counter radical (SG1: acyclic β-phosphonylated nitroxide, *N-tert*-butyl-*N*-(-1-diethylphosphono-2-2-dimethyl)propyl nitroxide [17]). Thereafter, the formation of polymer brushes is confirmed by confronting the experimental results for the structure of the polymer with the established theory. Moreover, the controlled behavior of this new approach is demonstrated for the first time with the SG1, used as a moderator agent, on elastomer polymer brushes (low glass transition = −55 °C). This approach was recently quoted as a recent advances in polymer brush synthesis by Brittain [18]. Finally, the conformational organization of the elastomeric macromolecular brushes in air is explored by AFM at room temperature, above the glass transition temperature.

2. Experimental section

2.1. Materials

Toluene was distilled under a nitrogen atmosphere from over molten sodium. SG1 counter-radical (Scheme 2(a)) and VAZO® 68 (4,4-azobis(4-cyanovaleric acid)) were used as received respectively from ATOFINA and DUPONT. All other solvents and chemicals products were purchased and used without further purification.

A one-sided polished Si(111) single-crystal wafer of 25.4 mm in diameter and 0.5 mm in thickness was purchased by Siltronix. The silicon wafers were treated in a piranha solution (H_2SO_4/H_2O_2, 7:3 by volume) for about 2 h at 120 °C to grow a thin native oxide layer to the surface. Thus, a surface of very low roughness (approximately 0.3 nm/μm^2) having a great reactivity (between 3 and 5 silanol functions per square nanometer) [19] was obtained. This treatment allows us to graft the coupling agent by condensation between the silanol functions (wafer surface) and the anchor groups of the coupling agent. The native oxide thickness was estimated at about 33 Å by ellipsometry measurement.

2.2. Characterizations and measurements

X-ray photoelectron spectroscopy (XPS) analyses were performed with a surface science instrument (SSI) spectrometer at room temperature, using a monochromatic and focused (spot diameter of 600 μm, 100 W) Al K_α radiation (1486.6 eV) under a residual pressure of 5×10^{-8} Pa. The hemispherical analyzer worked in constant pass energy mode, 50 eV for high resolution spectra and 150 eV for quantitative analysis. The binding energy scale was calibrated from the carbon contamination using the C(1s) line (284.6 eV) (a mean atomic percentage of 8% was determined).

Size exclusion chromatography (SEC) characterization was performed using a 2690 Waters Alliance System with THF as eluent equipped with four Styragel columns HR 0.5, 2, 4 and 6 at 40 °C in series with a 2410 Waters Refractive index detector and a 996 Waters Photodiode array detector. A calibration curve established with low polydispersity polystyrene standards was used for the determination of the polyacrylates molar masses.

Film thickness was measured with a UVISEL HR460 ellipsometer from JOBIN YVON. The conditions of measurements of the samples are as follows: incident angle of 70°, diameter of the beam of 500 μm and time of integration of 200 ms. Its spectral range is 0.73–4.75 eV (1700–261 nm). The following refractive indices were used for the various layers: 3.86 for native silicon, 1.46 for silicon oxide and 1.47 for poly(*n*-butyl acrylate) [10]. Measurements were obtained at three spots on each wafer, 10 measurements per spot. The uncertainty of the apparatus on the thickness measurements is 5 Å.

Force microscopy experiment were performed with the multimode scanning probe microscopy Nanoscope IV

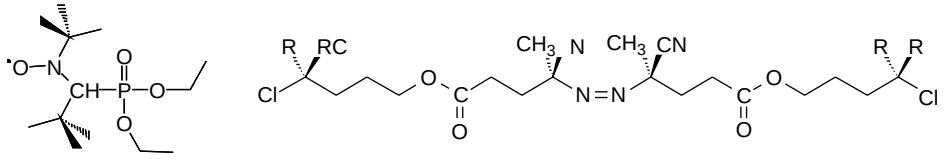

Scheme 2. Chemical structure of the SG1 stable counter-radical (a) and the coupling agents (b) ATCl (R = Cl) and AMCl (R = CH_3).

controller from Digital Instruments. For the AFM exploration the samples were in ambient air using the tapping mode (intermittent contact), while phase contrast images were used to detect sharp topographic changes.

2.3. Synthesis of functionalized azoic initiators

The azoic initiators (ATCl or AMCl; Scheme 2(b)) were obtained in three reaction steps according to the diagram followed by Rühe [20] for similar asymmetrical coupling agents: formation of the acid chloride from the corresponding azoic carboxylic acid (VAZO 68), esterification of the derivate with allyl alcohol and hydrosilation with a chlorosilane (mono or tri-functionalized) as we described for initiator-grafted silica particles [10,11].

2.4. Description of the hydrosilation reaction

Under dry nitrogen atmosphere, to a solution of 1 g (2.8×10^{-3} mol) of the allyl ester in 28 mL of the respective chlorosilane was added a solution of 30 mg of hexachloroplatinic acid in 6 mL of dimethoxyethane/ethanol (1:1, v/v), and the mixture was stirred 20 h. After that time all the solid dissolved, indicating the completion of the reaction. Dry toluene (50 mL) was then added and the excess of chlorosilane removed under reduced pressure. To remove residual platinum catalyst, the solution was then passed through a short column of dry sodium sulfate, the column was washed with dry dichloromethane, which was removed under reduced pressure. The toluene solution of the chlorosilyl derivate (ATCl or AMCl) was used without further purification; the concentration in coupling agent is estimated at approximately 60 mM.

2.5. Immobilization of the coupling agent [10,11,20]

Under an atmosphere of dry nitrogen, 1 mL of above solution of the crude chlorosilyl derivative (ATCl or AMCl) was added to the silicon wafer freshly cleaned in 5 mL of dry toluene. Pyridine (1 mL) was added drop-wise, and the reaction mixture was left to stand for overnight. The modified silicon wafer was then washed repeatedly with toluene, methanol and dichloromethane and then left to stand in dichloromethane for 18 h. This procedure was repeated to give the functionalized silicon wafers WMCl or WTCl.

2.6. Formation of polymer mono-layer

This part is essentially based on the results obtained from the surface-initiated NMP of *n*-butyl acrylate in presence of the SG1 silica particles [10]. To a reaction flask containing WMCl or WTCl was added a mixture of *n*-butyl acrylate, 2,2′-azobisisobutyronitrile (AIBN; [BA]/2[AIBN] = 400–1000) and SG1 (Scheme 2(a)-slight excess of 0.5% [9]: [SG1]/[AIBN] = 2.1 but a huge excess for the grafted azo initiator [SG1]/[*g*-Azo] = 2×10^{5}). Due to the small size of the wafer used in this study (≈1 cm^2), the amount of grafted azo initiator is neglected [*g*-Azo]/[AIBN] $\approx 10^{-5}$. This mixture was thoroughly degassed and heated to 120 °C for chosen periods of time. The silicon wafer was continuously washed free of any adsorbed polymer with toluene (good solvent of the polymer). Then the wafer was dried under nitrogen flux.

3. Results and discussion

3.1. Self-assembly of the initiator

The initiator used for this approach consists of an azoic group, which is structurally similar to AIBN and two chlorosilane head groups that connect the initiator through silanol moieties to the surface of the substrate. The coupling agents (Scheme 2(b)) was obtained from three reaction steps according to the diagram followed by Rühe [20] for similar asymmetrical coupling agents with exactly the same conditions as described in previous papers, on silica particles [10].

The Fig. 1(a) displays the XPS spectrum of the initiator layer. Two signals, due to the carbon (1s) (284.6 eV) and nitrogen (1s) atoms (400 eV), are characteristics of the azoic organic initiator. Indeed, in these experiments almost the whole C(1s) signal is due to the surface grafted initiator molecules.

Moreover, the deconvolution of the silicon (2p) signal (102.4 eV, Fig. 1(b)) in two peaks at 102.9 and 101.8 eV is an unambiguous proof of the presence of a grafted organic monolayer on the surface of the silicon wafer. Indeed, the dissymmetry of the peak related to the silica layer towards the low binding energies is characteristic of a covalent bond between the inorganic substrate and the organic compound

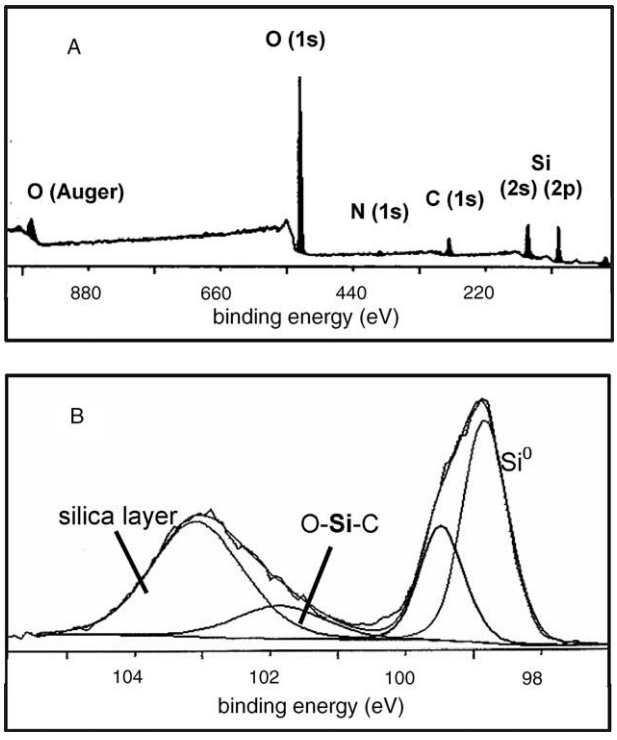

Fig. 1. Surface analysis by X-ray photoelectronic spectroscopy of silicon wafer with immobilized azoic coupling agent WMCl (A) and silicon peak (2p) deconvolution (B).

(O–Si–C, 101.8 eV). By comparing this one to the pure silicon signal (Si°, 98.4 eV), the thickness of the silica layer can be estimated at approximately 20–40 Å, thus confirming the result from ellipsometry measurements (cf. Section 2.1).

The initiator-grafted silicon wafers have also been characterized by ellipsometry to deduce the value of the grafting density σ_i (nm^{-2}), from the determination of the initiator (mono)layer thickness h according to Eq. (1), where N_a = Avogadro number (mol^{-1}), h = film thickness (nm), M = molecular weight ($g\,mol^{-1}$) and σ = relative density ($g\,nm^{-3}$).

$$\sigma = \frac{h\rho N_a}{M} \quad (1)$$

We report two principal characteristics of the organic initiator films deduced from the value of the (mono)layer thickness, h, and σ_i, describing the organic film thickness and the initiator grafting density, respectively.

For WMCl and WTCl, the organic film thicknesses h were determined to be 2.2 and 3.5 nm. These values correspond to different grafting densities of 2.8 and 5 mol/nm^2, respectively. If we compare these values with the original amount of silanol groups at the surface (treatment with piranha solution leads to: 3–5 silanol functions per square nanometer [19]), one notices that from 50 to 100% of these reactive groups had reacted under our experimental conditions. However, for the tri-functional initiator (WTCl), the grafting density obtained is too large to correspond really to a pure mono-layer. By comparing the uncertainty obtained (0.1 and 1, respectively for WMCl and WTCl), we can conclude that there is a significant difference in homogeneity of the initiator layers. In fact, these results are logical and could be interpreted by the formation of well-defined mono-layer for WMCl and multi-layer for WTCl due to the oligomerization of very reactive trichlorosilane functions. Moreover, using the same experimental conditions, structurally well-defined mono-layers of the initiator were obtained in a reproducible way by using AMCl (Scheme 2). Different samples of WMCl have been prepared with grafting densities varying between 2.6 and 2.8 mol/nm^2, that indicates a well-reproducible fabrication of patterned high density initiator grafted surfaces. The structural differences between the mono- and tri-functional silane can be seen in ^{29}Si solid-state NMR (CP-MAS technique) measurements on modified silica particles [10c,d].

Now, the presence of these initiator layers enables the synthesis of polymer brushes by surface-initiated NMP with a bimolecular system (SINMP): grafted azoic initiator and stable free radical SG1.

3.2. Formation of polymer brushes

The next step in preparation of polymer brushes consists in polymerization reaction of the acrylic monomer with the surface attached-initiator using the same approach as described in previous papers [10] for azoic initiator-grafted silica particles with the same bimolecular system. In the latter case, due to an extremely low concentration of initiating sites with respect to the monomer concentration, it was necessary to add predetermined amounts of free initiator (AIBN) to the reaction mixture to get in-situ polymerization [12a]. The addition of SG1, therefore, creates an overall concentration of nitroxide in the polymerization mixture, which controls the chain growth from both the immobilized and free initiators [10]. However, polymer chains formed in bulk of the solution due to addition of AIBN can be easily separated from the covalently bound polymer by washing the sample with an appropriate solvent. Thus, SEC characterization of the non-grafted polymers gives us an estimate for the molecular weight and polydispersity of the grafted polymers, if we assume that the polymerization behavior at the surface and in solution is similar. It should be stressed that the amount of the polymer grafted from the flat surface is extremely small; e.g. only 0.01 mg of the polymer corresponds to 100 nm thick film grown from a flat surface of 1 cm^2. Therefore, the analysis of molecular weight and polydispersity of the obtained grafted polymer chains by cleaving them from the surface as it has been done with high specific surface area substrates using the ester function (Scheme 2) of the grafted initiator [10,20] is not possible in our case.

Fig. 2 displays XPS spectra of a PBA mono-layer; the spectrum B illustrates the composition of the wafer composed of about 4 nm thick PBA mono-layer (M_n(freePBA) = 3700 g/mol, $M_w/M_n = 1.26$) for the samples prepared from the mono-functional agent (WMCl).

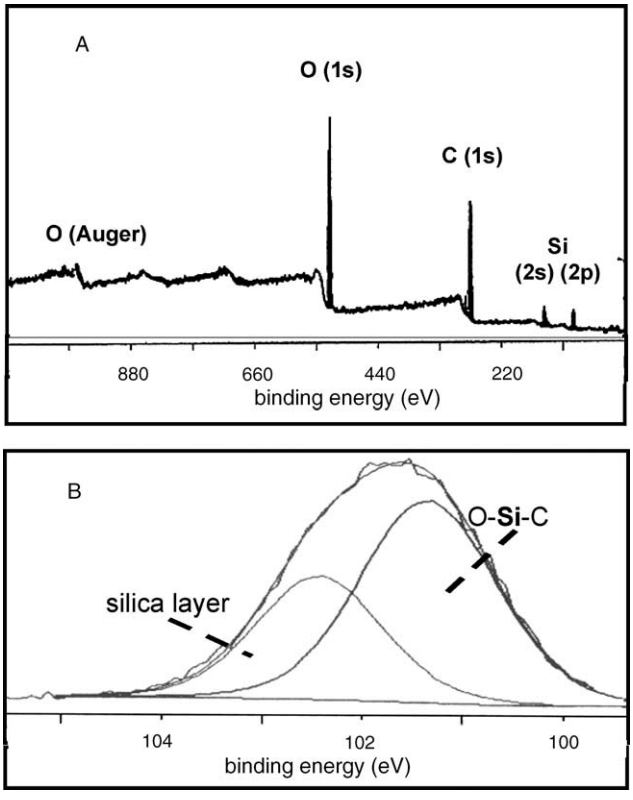

Fig. 2. Surface analysis by X-ray photoelectron spectroscopy of silicon wafer with immobilized azoic coupling agent WMCl (A) and silicon peak (2p) deconvolution (B). $M_n = 3700$ g/mol $M_w/M_n = 1.26$.

Table 1
Grafting density σ_p, thickness h and stretch S of PBA mono-layers

	WMCl-PBA1	WTCl-PBA1	WTCl-PBA2
[BA]/[AIBN]	400	400	400
Time (h)	1.5	2.5	3.5
Conversion (%)	8	25	45
M_n[a] (M_w/M_n)	3700 (1.26)	14,000 (1.12)	20,700 (1.1)
h (nm)	4.1±0.1	11.5±0.2	14.0±0.2
σ_p (chain/nm^2)	0.70±0.05	0.50±0.01	0.40±0.05
S (±0.05)	0.63	0.43	0.35
R_g/L	0.41	0.19	0.15

[a] g/mol (free polymer).

The comparison of this spectrum with the XPS spectrum of the coupling agent mono-layer (WMCl-Fig. 1(A)) shows a strong enhancement of the carbon C(1s) signal at 286.5 eV. Additionally, the signals of silicon peaks are attenuated, and the C(1s)/O(1s) and C(1s)/Si(2p) signals ratio are clearly enhanced, demonstrating the presence of the organic polymer on the surface. Thereafter, comparison of silicon (2p) spectra (Figs. 1(B) and 2(B)) shows a shift of the signal characteristic of the native oxide layer towards the low binding energies (102.8–102.3 eV). This result confirms the formation of an organic polymer mono-layer grafted on the silicon wafer surface by covalent bound links.

The silicon wafers modified by grafted polymer chains have also been characterized by ellipsometry to deduce the value of the grafting density σ_p from the determination of the polymer mono-layer thickness h according to Eq. (1) ($\rho = 1.014$ g/cm^3 for poly(*n*-butyl acrylate)) [21]. Table 1 presents results for different PBA films obtained from WMCl and WTCl.

From the values of the grafting densities σ_p obtained, we notice that they are significantly smaller than the values obtained for the corresponding initiator. Thus, only a small fraction of the grafted initiator was activated during the surface-initiated NMP. A efficiency of initiation can be estimated around 25 and 10% for WMCl and WTCl, respectively. In fact, σ_p was calculated using parameters (density and molecular weight) obtained for free polymers. The neutron reflectivity experiments by Devaux [13c] on polystyrene brushes (silicon wafers) in air atmosphere indicate that the scattering length density increases with increasing degree of stretching of polymer chains in the brush. Thus, we can suppose that the density of the grafted polymer layer is higher than that of a dry polymer in the bulk and increases upon an increase in the grafting density of macromolecular chains. The slower growth of the chains from the surface as compared to that in solution can be attributed to geometric constraints resulting from high surface density of the chains. In spite of polymerization under constrained conditions, few examples demonstrated the formation of polymer brushes by NMP with controlled molecular weight and narrow polydispersities [10c,12a,13]. The lower efficiency of initiation of polymerization from the surface as compared to that in the bulk has been previously described for similar bimolecular system on silica particles [10] or commonly observed with different types of initiator for CRP [2,3,12–14]. Nevertheless, the values of the grafting density are still high and for high molecular weights the grafted polymer mono-layers are in a so-called brushes regime ($0.4 < \sigma_p < 0.7$ chain/nm^2). Indeed, for the lowest molecular weight ($M_n = 3700$ g mol^{-1} with $M_w/M_n = 1.26$) the calculated value of R_g is 2.43 nm, while the surface area per one chain is around 1.42 nm^2 (corresponding to grafting density $\sigma_p = 0.7$ nm^{-2}). At the same time, for the highest molecular weight ($M_n = 20{,}700$ g mol^{-1}), the gyration radius R_g is 5.75 nm whereas the area per chain is 2.5 nm^2. For these two dimensions of grafted chains, the grafting density σ_p is much higher than that corresponding to the overlap of chains, confirming occurrence of a brushes regime.

When each grafted initiator is active and propagates simultaneously, the geometric constraints imposed on a chain by its neighbors force the macromolecule to adopt an extended conformation. According to the molecular weights of chains grown in solution and a repeat unit (C–C bond) length of 2.5 Å, a comparison between the measured film thickness and the contour length of polymers can be made. The results from this study indicate that the measured thickness is lower than the values calculated for the contour length, as expected. Using this two values it is possible to calculate the degree of stretching S of the grafted polymer chains (Eq. (2): Lth(PBAgref) = N(PBAfree)×lab with N = degree of polymerization and lab = 0.25 nm (monomer unit length)) as

$$S = \frac{h}{Nl_{ab}} \tag{2}$$

Moreover, for each degree of polymerization, S is always higher than the value of the ratio R_g/L (where R_g is the radius of gyration [23] of a free polymer chain in solution and L is theoretical contour length for a totally extended chain), Table 2. Hence, due to packing condition (for the dry state in air) and crowding ($2R_g$ is always higher than D, distance between two grafted chains) the polymer chains are extended in the direction perpendicular to the surface, $h > R_g$.

For different sets of polymerization, we have observed a linear variation of the thickness of the grafted polymer mono-layers as a function of molecular weight (determined by GPC for free polymers) for a wide range of molecular weight and with time of polymerisation, as respectively, described in Fig. 3(b) and (c).

Table 2
Grafting density σ_p, thickness h and stretch S of PBA mono-layers after re-initiation

	WMCl-PBA3	WMCl-PBA4	WTCl-PBA3
$M_{n,initial}$ (g/mol)	3700	3700	14,000
[BA]/[AIBN]	1000	1000	1000
Time (h)	2	6	3
Conversion (%)	20	65	30
$M_{n,final}$ (g/mol)[a]	26,000	86,000	45,600
h (nm)	16.5±0.5	30±3	25.4±1.5
σ_p (mol/nm^2)	0.40±0.05	0.20±0.03	0.34±0.05
S ($S_{initial}$)	0.33 (0.63)	0.18 (0.63)	0.30 (0.43)

[a] $M_{n,final} = M_{n,initial} + M_{n,re\text{-}initation}$ (free polymer) obtained by SEC with PS calibration.

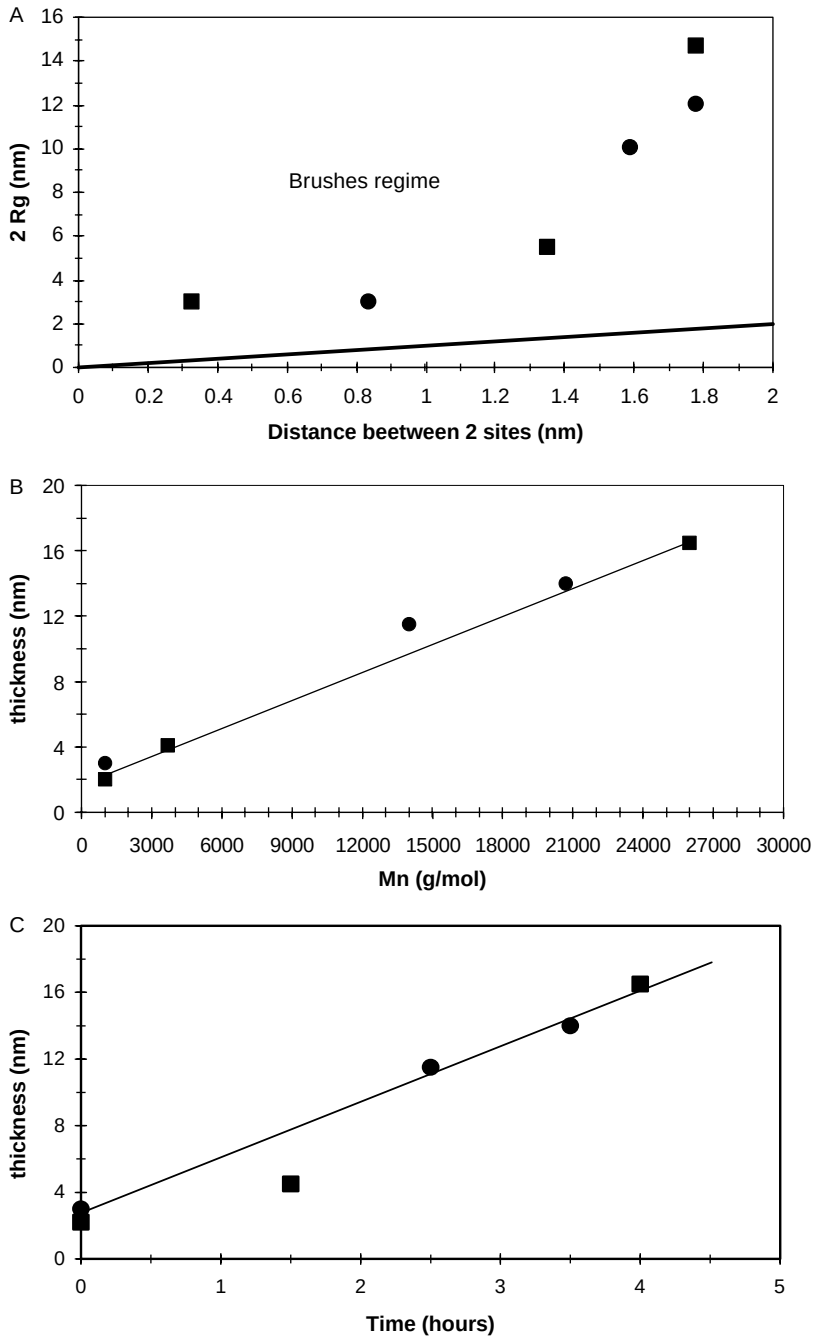

Fig. 3. (A) Variation of the radius of gyration R_g of the free polymer with the distance D (initiator to *n*-butyl acrylate molar ratio = 400; black line = polymer brushes limit), (B) variation of the thickness of the polymer film with the molecular weight of the free macromolecular chains, (C) variation of the thickness of the polymer film with time of polymerisation: black squares WMCl-PBA and black circles WTCl-PBA.

This linear variation indicates conservation of the number of growing chains generated from the surface. Therefore, we can conclude that the surface-initiated NMP from the initiator grafted on silicon wafer surfaces has a controlled character.

3.3. Re-initiation of free and grafted polymers

Remarkably, the presence of the nitroxide SG1 at the chain ends gives us the opportunity to elaborate block copolymers with antagonist properties grafted at the surface as we have previously described for silica particles [24]. The presence of the nitroxide SG1 at the end of the grafted polymer chains can be observed by XPS with two new signals due to phosphorus (2p) and nitrogen atoms (1s), respectively, at 133.7 and 402 eV (Fig. 4).

An alternative goal of this study was to control the ability of the SINMP to re-initiate the growth of PBA macromolecular chains grafted on a flat surface. In order to verify the living/controlled character of polymerization, we have synthesized a free polymer (PBA1) at 120 °C in presence of MONAMS (alkoxyamine used as an initiator for NMP [25]) and with a slight excess of SG1 (5%). After purification and

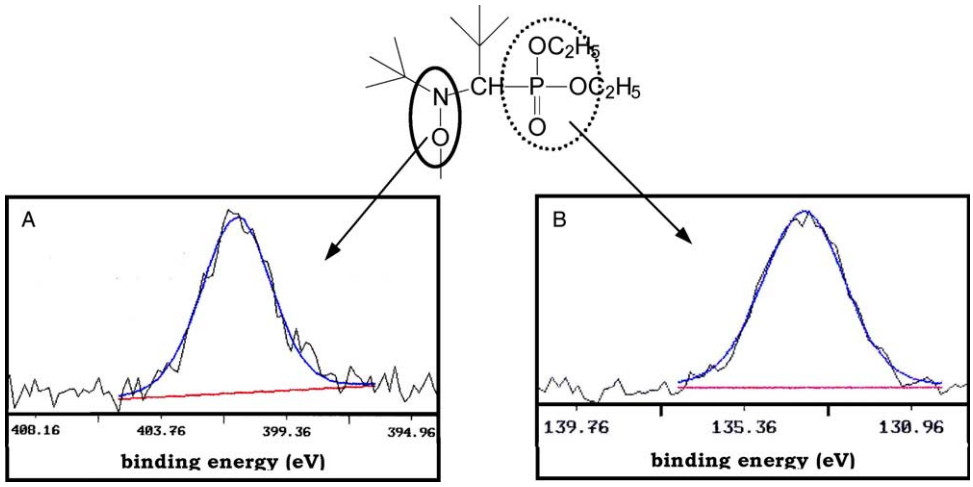

Fig. 4. Surface analysis by X-ray photoelectron spectroscopy of silicon wafer with PBA brush: (A) nitrogen peak N(1s) at 402 eV and (B) phosphorus peak P(2p) at 133.7 eV. (M_n = 3700 g/mol M_w/M_n = 1.26)

characterization (^{1}H NMR and SEC), PBA1 was re-initiated at 120 °C in presence of *n*-butyl acrylate monomer; PBA1 plays the role of macro-initiator due to the presence of a SG1 in the end chains. Then the polymer obtained by re-initiation of the nitroxide mediated polymerization, PBA2 was characterized by SEC. In Fig. 5, the comparison of the two chromatograms A and B shows an increase in the molar mass of the polymer proving that the re-initiation has taken place. In this case, just a simple comparison indicates that only few percents of the SG1 end-capped PBA have not initiated the second polymerization, those chains are commonly called 'dead' chains (<5%) [26]. Hence, re-initiation can be performed by NMP, via a re-activation of the SG1 end-capped polymer, with a good control over the macromolecular dimensions of the two segments and with narrow polydispersity. A second re-initiation was made with the same conditions as the first one and 35% of the 'dead' chains are calculated by deconvolution (Fig. 5(C)).

From these results, we can conclude that the first re-initiation can be performed (I_p = 1.15) and the second one considered, under controlled conditions (I_p = 1.28). This approach was applied to re-initiation of PBA chains grafted on silicon wafers, in order to demonstrate the ability to re-initiate the dormant species at the end of macromolecular chains grafted from the flat surface.

The results of the re-initiation are resumed in Table 2. From the initial WMCl wafer the molecular weight increases strongly and at the same time a significant increase in the film thickness is observed. Indeed, the evolution of the molecular weight from 3700 to 86,000 is responsible for the increase in the thickness from 4 nm (initial state) to 30 nm (one after re-initiation). The same behaviour is observed for WTCl wafer with the same order of magnitude and in both cases, the values of the grafting density σ_p and the degree of stretching *S* are slightly lower.

However, the aim of this study was to confirm the influence of the re-initiation on the thickness of the polymer brushes (Fig. 6(b)). Another important question is whether re-initiated chains do overlap, i.e. the polymer layer obtained by re-initiation of polymerisation remains in the brush regime (Fig. 6(a)). In Fig. 6(b), we have represented the evolution of the thickness of the polymer film due to the re-initiation. In this case, we have observed a significant increase (up to 30 nm) in the thickness of the layer versus the molecular weight of the grafted chains. However, after re-initiation, the evolution of the thickness as a function of molecular weight of polymer chains is different from that observed for the initial polymerization stage.

Indeed, the slope of the brush thickness versus degree of polymerization dependence after re-initiation is noticeably smaller than that observed for initial polymerization (Fig. 6(b), black line). This aspect is due to the loss of active centers at the end of some grafted chains. Similar phenomenon has been previously described for free polymer chains (Fig. 5).

Nevertheless, one of the most important aspect of this study was to confirm the maintenance of brushes regime after one re-initiation and an increase in the molecular weight of grafted chains due to the specific behaviour of the CRP. In Fig. 6(a), we have plotted the radius of gyration $2R_g$ versus average distance

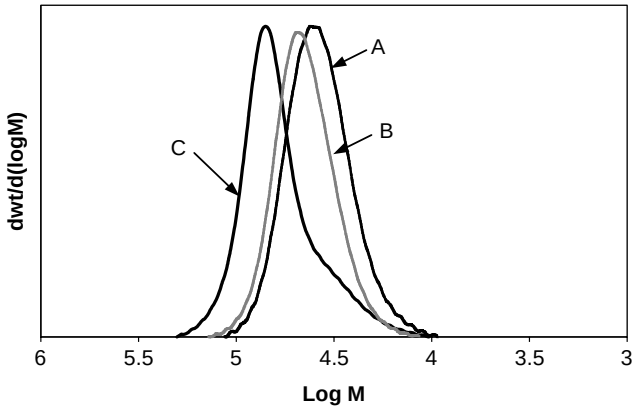

Fig. 5. MWD curves for NMP of BA using (A) MONAMS as initiator at 120 °C in bulk with [BA]/[MONAMS] = 650 (M_n(PBA1) = 35,000 g/mol and M_w/M_n = 1.15) (B) PBA1 as macro-initiator at 120 °C in bulk (M_n(PBA2) = 41,300 g/mol and M_w/M_n = 1.15) (C) PBA2 as macro-initiator at 120 °C in bulk (M_n(PBA3) = 51,350 g/mol and M_w/M_n = 1.28).

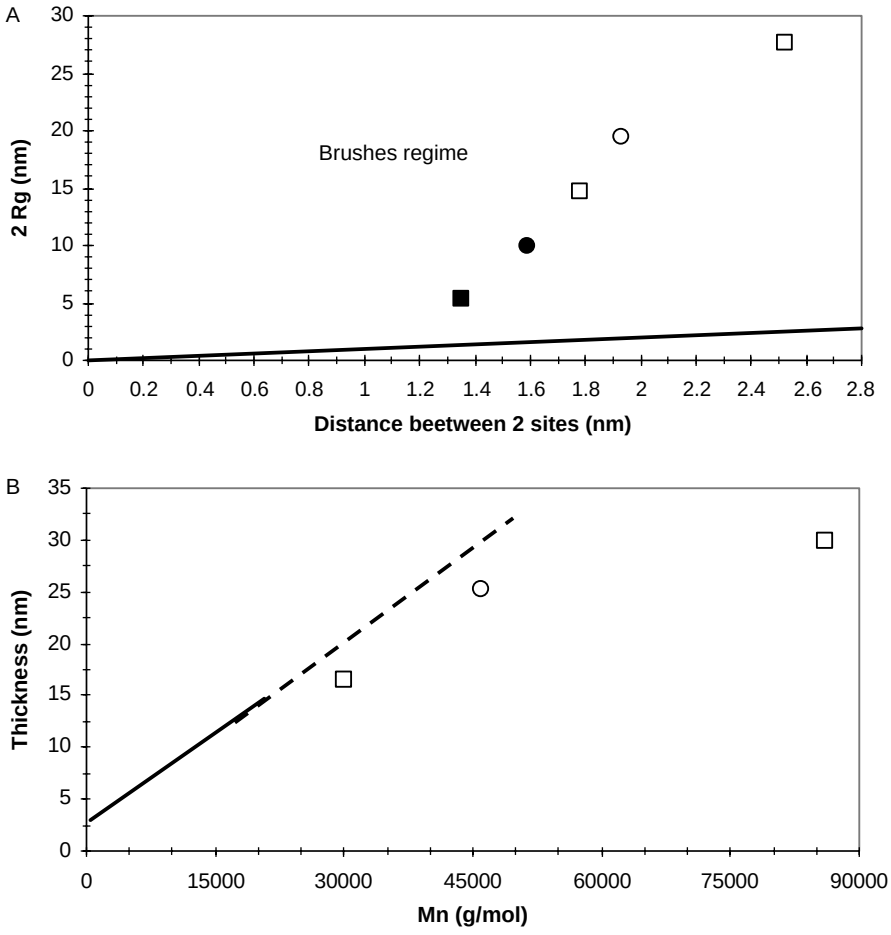

Fig. 6. (A) Variation of the radius of gyration R_g of the free polymer with the distance D, initial chains (black symbols) and re-initiated chains (white symbols) (black line = polymer brushes limit), (B) variation of the thickness of the polymer film with the molecular weight of the free macromolecular chains: initial chains (black line), total efficiency of re-initiation (dash line) and re-initiated chains (white symbols).

between two neighboring grafted macromolecular chains for different samples synthesized in this work. This representation clearly demonstrates, that the polymer brushes regime is conserved and even re-inforced after re-initiation even in spite of the increase in the distance between two grafted chains. Indeed, the larger distance between neighbouring grafted chains is overcompensated by larger gyration radius due to higher molecular weight [22]. Since $2R_g/D$ is large than unity, one can conclude that the polymer layer remains in the brush regime over the wide range of variation of the molecular weight of grafted chains (Fig. 7).

3.4. Atomic force microscopy

For the system of polymer chains end-grafted to a planar surface and collapsed in the dry state or in poor solvent, different possible structural organizations on the surface have been predicted theoretically [27]. For instance, lateral micro-phase segregation may occur via the formation of pinned micelles.

Comparing the free energies per chain in a micelle and in other possible structures (separate single chains and homogeneous grafted layer), one finds that pinned micelles are stable in the range of grafting densities

$$l_{ab}^{-2}N^{-4/3} \cong \sigma_{pI} \leq \sigma_p \leq \sigma_{pII} \cong l_{ab}^{-2}N^{-1/2} \quad (3)$$

At $\sigma_p \ll \sigma_{pI}$, the chains form individual single-chain pinned globules whereas, at $\sigma_p \gg \sigma_{pII}$ the pinned micelles coalesce into a homogeneous grafted layer. Such a phenomenon has

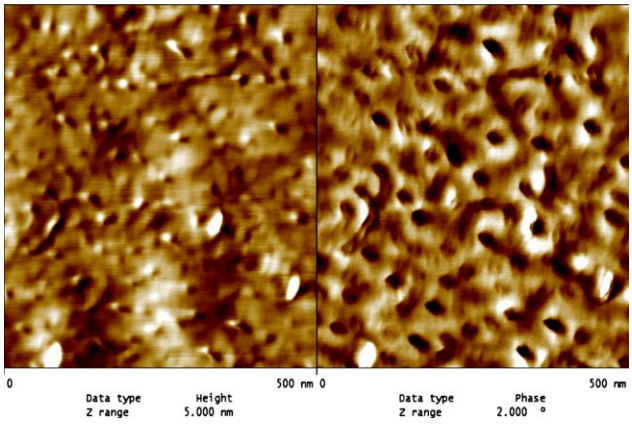

Fig. 7. AFM image of polymer brushes of PBA grafted on silicon wafer WMCl-PBA1 ($M_n = 3700$ g/mol $M_w/M_n = 1.26$).

been experimentally demonstrated by Koutsos et al. [28] for polystyrene chains end-grafted onto gold surface.

An AFM image of a grafted PBA mono-layer is presented in Fig. 7. The holes observed on the extreme surface could be associated to the presence of pinned micelles or other type of nano-segregated structures.

For the degree of polymerization of the PBA grafted is around 26 (M_n = 3700) the calculated from the thickness measurements grafting density is σ_p = 0.7 chain/nm^2. Hence, one can conclude that the degree of overlapping of the chains in the layer is relatively small (near the limit of the brush regime). Particularly under these conditions, one can expect appearance of individual pinned globules or/and pinned micelles in the dry (collapsed) state. The formation of nano-patterned structure due to re-arrangement of the grafted chains conformations upon drying should be facilitated due to high local mobility of the chain segments ('soft' brush) at room temperature ($T_g \approx -55$ °C for free chains). Indeed, if several authors reported recently that the properties (e.g. glass transition temperature) of polymer brushes grafted on the solid surfaces are different from those of ungrafted chains [29–31], we have also demonstrated a glass transition temperature increase in 20 °C for the poly(butyl acrylate) PBA brushes on silica particles, i.e. $T_g = -35$ °C [24]. A study by ellipsometry is underway in order to estimate the effect of the conformation of the grafted chains on flat surface, i.e. grafting densities, to the value of T_g. But at this stage, we can assume that the PBA brushes is still in an elastomer regime, the value of T_g being still under room temperature, where the chains local mobility is high.

Moreover, Reiter has described the dewetting phenomena in thin adsorbed polymer films as a macroscopic manifestation of the instability of films describing the local mobility of the chains at interfaces [32]. The dewetting of the film was traduced by the apparition of some irregularities on the thickness profile of the thin layer. The presence of such a transformation in the morphology of layers at temperature lower than T_g in the bulk polymers was interpreted by Reiter as an increase in the chains mobility at the surface due to a decrease in the T_g in the film. In order to hinder the dewetting, some authors propose to introduce long chains to increase the entanglements (physical links) and stabilize the film [32–35].

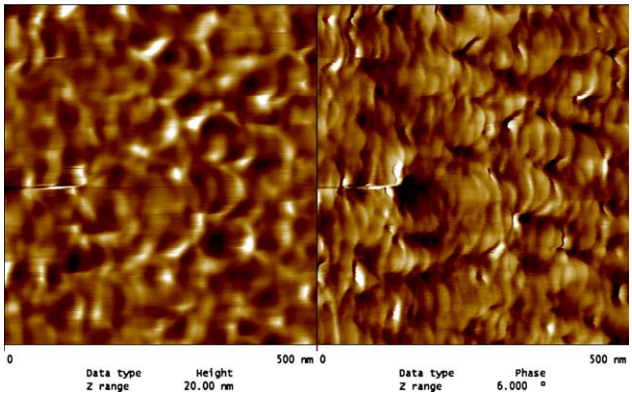

Fig. 8. AFM image of polymer brushes of PBA grafted on silicon wafer WMCl-PBA4 (M_n = 86,000 g/mol).

In our case an increase in the molecular weight of grafted chains (up to 86,000 g mol^{-1}, the corresponding film thickness 30 nm) has been achieved after re-initiation of the previous wafer WMCl-PBA1 (corresponding sample WMCl-PBA4 Table 3). After this re-initiation, a more homogeneous film is obtained without any appearance of dewetability of the film on the extreme surface (Fig. 8). This lateral homogeneity can be explained by (a) larger degree of overlapping of the chains in the brush, i.e. weaker tendency for equilibrium micro-phase separation and (b) lower mobility of longer chains in the brush.

4. Conclusion

We have demonstrated that well-defined 'soft' (elastomer) PBA brushes on silicon wafers can be prepared by surface-initiated NMP using the bimolecular system azoic initiator/SG1 counter radical. The chain growth process from the initiator-grafted silica surface leads to polymer monolayers which exhibit all the features of the polymer brushes, i.e. strong crowding of neighboring grafted chains, extension of the chains in the direction perpendicular to the grafting surface with respect to the Gaussian dimensions. Using this graft from procedure, the nature and composition of the polymer monolayer (chemical structure, chain length, and grafting density) can be precisely controlled and adjusted, which is of major importance for specific applications. Under bimolecular NMP conditions, linear increase in the monolayer thickness as a function of the molecular weight of the free polymer demonstrates the controlled radical polymerization character of the chain growth process, i.e. the preservation of chain functionality. Moreover, confirmation of the effectiveness of the NMP process has been realized through XPS characterization and re-initiation of chain growth of polyacrylate monolayers with the same monomer (reactivation). Thus, it should be possible to tune the surface properties (for instance the adherence, wettability…) of the inorganic material by choosing the nature (elastomeric, thermoplastic, hydrophilic…) and the dimension of an adequate grafted polymer or diblock copolymer. This opens a large perspective for design of polymeric mono-layers with pre-determined and responsive features adjustable for different applications.

Acknowledgements

The authors are pleased to acknowledge O. Guerret from ATOFINA for supplying SG1. Mr Maurice Brogly, Laurent Vonna (Institut de Chimie des Surfaces et Interfaces, Mulhouse, France), Mrs Marchand and Mr Gaston from JOBIN YVON (France) are acknowledged for their helpful for ellipsometry measurements.

References

[1] (a) Fisher H. J Am Chem Soc 1986;108:3925.
(b) Fisher H. Macromolecules 1997;30:5666.
[2] (a) Chen X, Randall DP, Perruchot C, Watts JF, Patten TE, von Werne T, et al. J Colloid Interface Sci 2003;257:56.

(b) von Werne T, Patten TE. J Am Chem Soc 2001;123:7497.
(c) Perruchot C, Khan MA, Kamitisi A, Armes SP, von Werne T, Patten TE. Langmuir 2001;17:4479.
(d) von Werne T, Patten TE. J Am Chem Soc 1999;121:7409.
[3] (a) Boettcher H, Hallensleben ML, Wurm XX. Polym Bull (Berlin) 2000; 44:223.(b) Boettcher H, Hallensleben ML, Wurm H. DE 19838241; 1998.
[4] (a) Matyjaszewski K. Macromol Symp 2001;174:51.
(b) Matyjaszewski K, Miller P, Shukla N, Immaraporn B, Gelman A, Luokala B, et al. Macromolecules 1999;32:8717.
(c) Matyjaszewski K. Curr Opin Solid State Mater Sci 1996;1:769.
(d) Matyjaszewski K. J Phys Org Chem 1995;8:197.
[5] Beckwith ALJ, Bowry VW, O'Leary M, Moad G, Rizzardo E, Solomon DHJ. Chem Soc, Chem Commun 1986;32:1003.
[6] Georges M, Veregin R, Kazmaier P, Hamer G. Macromolecules 1993;26: 2987.
[7] Benoit D, Grimaldi S, Finet JP, Tordo P, Fontanille M, Gnanou Y, et al. Polym Prepr, ACS Polym Div 1997;38:651.
[8] Gnanou Y, Robin S, Guerret O, Couturier JL. Polym Prepr 2000;41:1352.
[9] (a) Lacroix-Desmazes P, Lutz JF, Boutevin B. Macromol Chem Phys 2000;201:662.
(b) Lacroix-Desmazes P, Lutz JF, Chauvin F, Severac R, Boutevin B. Macromolecules 2001;34:8866.
[10] (a) Parvole J, Billon L, Montfort JP. Polym Int 2002;51:1111.
(b) Parvole J, Montfort JP, Billon L. Macromol Chem Phys 2004;205: 1369.
(c) Parvole J, Laruelle G, Khoukh A, Billon L. Macromol Chem Phys 2005;206:372.(d) Parvole J. Thesis of Pau University; 2003.
(e) Inoubli R, Dagreou S, Roby F, Khoukh A, Peyrelasse J, Billon L. Polymer 2005;46:2486.
[11] Parvole J, Laruelle G, Guimon; C, Francois J, Billon L. Macromol Rapid Commun 2003;24:1074.
[12] (a) Husseman M, Malmström EE, McNamara M, Mate M, Mecerreyes D, Benoit D, et al. Macromolecules 1999;32:1424.
(b) Husseman M, Morrison M, Benoit D, Frommer J, Mate C, Hinsberg W, et al. J Am Chem Soc 2000;122:1844.
(c) Blomberg S, Ostberg S, Harth E, Bosman AW, van Horn B, Hawker CJ. J Polym Sci, Part A: Polym Chem 2002;40:1309.
[13] (a) Bartholome C, Beyou E, Bourgeat-Lami E, Chaumont P, Zydowicz N. Macromolecules 2003;36:7946.
(b) Bartholome C, Beyou E, Bourgeat-Lami E, Chaumont P, Lefebvre F, Zydowicz N. Macromolecules 2005;38:1099.(c) Devaux C. Thesis of University of Lyon I; 2001.
[14] Kasseh A, Ait-Kadi A, Riedl B, Pierson JF. Polymer 2003;44:1367.
[15] Halperin A, Tirrell M, Lodge TP. Adv Polym Sci 1991;100:39.
[16] Sonnenberg L, Parvole J, Borisov O, Billon L, Gaub HE, Seitz M. Macromolecules 2006;39:281.
[17] Grimaldi S, LeMoigne F, Finet JP, Tordo P, Nicol P, Plechot M, et al. European Patent 0832902 A2; 1998.
[18] Advincula RC, Brittain WJ, Caster K, Ruhe J, editors. Polymer brushes. Weinheim: Wiley–VCH; 2004. p. 35.
[19] Iler RK, editor. The chemistry of silica. New York, NY: Wiley; 1979.
[20] (a) Prucker O, Rühe J. Macromolecules 1998;31:592.
(b) Prucker O, Rühe J. Macromolecules 1998;31:602.
(c) Prucker O, Rühe J. Langmuir 1998;14:6893.
[21] Brandrup J, Immergut EH, editors. Polymer handbook. New York, NY: Wiley; 1989.
[22] Jones DM, Brown AA, Huck TS. Langmuir 2002;18:1265.
[23] $R_g = 0{,}04 \times Mw^{0.5}$.
[24] Laruelle G, Parvole J, Francois J, Billon L. Polymer 2004;45:5013.
[25] Couturier JL, Henriet-Bernard C, Le Mercier C, Tordo P, Lutz JF. Patent WO 00/49027, ElfAtochem SA; 24 August 2000.
[26] Benoit D, Grimaldi S, Robin S, Finet JP, Tordo P, Gnanou Y. J Am Chem Soc 2000;122:5929.
[27] (a) Williams DRM. J Phys II (France) 1993;3:1313.
(b) Zhulina EB, Birshtein TM, Priamitsyn VA, Klushin LI. Macromolecules 1995;28:8612.
[28] (a) Koutsos V, van der Vegte EW, Pelletier E, Stamouli A, Hadziioannou G. Macromolecules 1997;30:4719.
(b) Koutsos V, van der Vegte EW, Hadziioannou G. Macromolecules 1999;32:1233.
[29] Urayama K, Yamamoto S, Tsuji Y, Fukuda T, Neher D. Macromolecules 2002;35:9459.
[30] Tanaka K, Kojio K, Kimura R, Takahara A, Kajiyama T. Polym J 2003; 35:44.
[31] Tate RS, Fryer DS, Pasqualini S, Montague MF, De Pablo JJ, Nealey PF. J Chem Phys 2001;115:9982.
[32] (a) Reiter G. Langmuir 1993;9:1344.
(b) Sharma A, Reiter G. J Colloid Interface Sci 1996;178:383.
(c) Reiter G. Macromolecules 1994;27:3046.
[33] Yuan C, Ouyang M, Koberstein J. Macromolecules 1999;32:2329.
[34] Henn G, Bucknall DG, Stamm M, Vanhoorne P, Jerome R. Macromolecules 1996;29:4305.
[35] Barnes KA, Karim A, Douglas JF, Nakatani AI, Gruell H, Amis EJ. Macromolecules 2000;33:4177.